Time optimal control of gearbox synchronizers for minimizing noise and wear

Citation for the original published paper (version of record):

Piracha, M., Grauers, A., Hellsing, J. (2020). Time optimal control of gearbox synchronizers for minimizing noise and wear. CCTA 2020 - 4th IEEE Conference on Control Technology and Applications: 573-580. http://dx.doi.org/10.1109/CCTA41146.2020.9206254

2020 IEEE Conference on Control Technology and Applications (CCTA)
August 24-26, 2020. Montréal, Canada

Time optimal control of gearbox synchronizers for minimizing noise and wear

Muddassar Zahid Piracha
Automatic Control, Electrical Eng
Chalmers University of Technology
Powertrain Concept, CEVT AB
Sweden
muddassar.piracha@cevt.se

Anders Grauers
Automatic control, Electrical Eng.
Chalmers University of Technology
Sweden
anders.grauers@chalmers.se

Johan Hellsing
Powertrain Concept, CEVT AB
Sweden
johan.hellsing@cevt.se

***Abstract*— Hybrid dual clutch transmissions can reduce fuel consumption and CO_2 emissions significantly at a low cost, but they will lead to torque interrupt shifts in electric vehicle mode. To improve the shift quality, the shift time should be minimized and the impacts between the sleeve teeth and the idler gear dog teeth after speed synchronization should also be minimized. Besides creating noise, these impacts are also responsible for delaying the completion of shift and contribute to wear in the dog teeth. This paper presents a time optimal control strategy for mechanical synchronizers in a hybrid dual clutch transmission, which includes constraints such that impacts between sleeve and gear dog teeth are minimized. It is demonstrated how a mechanical synchronizer can be modeled as a double integrator system and how the standard time-optimal control solution of double integrator system must be modified such that it can be applied to mechanical synchronizers. The result is a feedback control strategy that guarantees minimum speed synchronization time and minimum noise/wear in transmission. The performance of the controller is verified by simulation.**

Keywords*— *Hybrid Powertrain, Dual Clutch Transmission, Mechanical Synchronizers, Optimal Control

I. INTRODUCTION

The transmission studied in this paper is a 7-speed hybrid dual clutch transmission (7DCTH). In electric vehicle mode (EV mode), when both clutches C1 and C2 are open and the combustion engine is off, is shown in the schematic diagram in Figure 1. The electric motor (EM) will be driving the vehicle via even gears as shown by the yellow line representing the power flow. So, in EV mode the rest of the system can be ignored. The important part of the driveline in EV mode is shown in Figure 2, including the gear shift mechanism with synchronizers.

Before gear shift, sleeve will be connected to offgoing idler shown in pink in Figure 2, so EM will drive the wheels via input shaft, offgoing idler, sleeve and output shaft. When the shift is ordered the sleeve must be disconnected from offgoing idler and connected to the oncoming idler shown in red in Figure 2. From Figure 2 it can be seen that since both oncoming idler and offgoing idler are on the same shaft, the shift will always be a ‘‘Torque Interrupt shift’’. A torque interrupt shift can be defined as a shift where during shift the wheels are disconnected from torque source, i.e. the electric motor for a hybrid vehicle in EV mode. Consequently, driver does not get the requested torque and unwanted changes in acceleration are felt. So, in order to maintain good drivability, the shift time of torque interrupt shifts must be minimized. A torque interrupt shift has the following five phases [1] and the total shift time is from the start of phase 1 until the end of phase 5 [2].

1. Torque ramp down
2. Sleeve to Neutral
3. Speed Synchronization
4. Sleeve to Gear Engagement
5. Torque Ramp up

At the beginning of the gear shifting, during torque ramp down phase, driving torque from traction EM is removed from off going idler gear. Once the driving torque is zero, sleeve to neutral phase begins, where sleeve is disengaged from offgoing idler and moved to the neutral position shown in Figure 2.

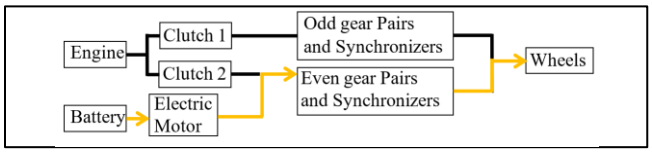

Figure 1 Layout of 7DCTH and its EV mode

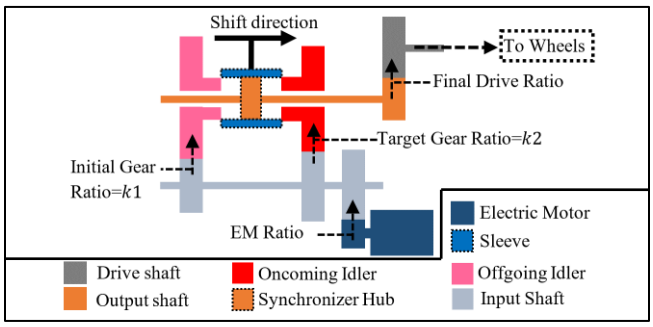

Figure 2 Driveline in EV mode

In speed synchronization phase the rotational velocity of oncoming idler is matched with that of sleeve. This can be achieved by different methods as shown in [1]. Once the speed difference between oncoming idler and sleeve is zero, sleeve to gear engagement phase starts where sleeve is

978-1-7281-7140-1/20/$31.00 ©2020 IEEE

pushed to engage with oncoming idler. After sleeve has moved a certain distance on the oncoming idler driving torque from traction EM is resumed and shift is finished.

Phase 3, the speed synchronization phase, takes the longest percentage of the complete shift time, and to reduce shift time significantly, synchronization time must be minimized.

During Phase 4, the sleeve to gear engagement, there are often impacts between sleeve teeth and oncoming idler gear dog teeth [3]. These impacts are responsible for noise during gear shifts. Additionally, these impacts are also responsible for shortening the life span of transmission [3]. So, to minimize noise and wear in transmission during the gear shifting these impacts must be minimized.

In the existing methods, only the time for speed synchronization phase is minimized, this paper deals with time optimal control to reduce both the speed synchronization time and the impacts between sleeve teeth and oncoming idler gear dog teeth.

Section II describes the geometry of synchronizer and its modeling. The dog teeth position sensor explained in [4] is also introduced in this section. Section III describes the speed synchronization between sleeve and idler gear in detail. Section IV relates the conditions at the end of speed synchronization with the analysis in [4] to formulate the conditions necessary to avoid impacts between sleeve teeth and oncoming idler gear dog teeth. The Dog teeth position sensor presented in [4] is also discussed in the context of feedback control implemented in later sections.

In Section V speed synchronization is formulated as a Time optimal control problem and is solved using the approach in [5]. The resulting Time Optimal control sequences are studied in the context of synchronizers. Switching Curve necessary for application of time optimal feedback control is derived and simulation results shows a gear shift with this controller.

II. Mechanical Synchronizer

A side view of a mechanical synchronizer is shown in Figure 3. The components in speed synchronization are sleeve, blocker ring and oncoming idler gear as shown in the assembly view in Figure 3.

Analysis of synchronizers becomes very convenient when each individual component is represented by its dog teeth as shown Figure 4. The dog teeth of sleeve, blocker ring and idler gear are shown when synchronizer is in neutral.

The teeth geometry is also shown in Figure 4. The dog teeth width for all teeth is w_{dog} and the half angle of teeth tip is β. The sleeve tip position y_s and idler gear tip position y_g can be measured by using the ''Dog teeth position sensor'' which is explained in detail in [4].

The relative alignment between sleeve and idler gear dog teeth y_{sgr} will be used as feedback signal for the control algorithm, so its bounds will affect the controller design. The bounds are discussed here and the effects on controller design are discussed in later sections of this paper.

y_{sgr} at any time instance t_i can then be calculated using

$$y_{sgr}(t_i) = \begin{cases} y_g(t_i) - y_s(t_i) & \text{if } y_g(t_i) > y_s(t_i) \\ y_{sg}max - y_s(t_i) + y_g(t_i) & \text{if } y_s(t_i) > y_g(t_i) \end{cases} \quad (1)$$

where $y_{sg}max$ is the distance between two consecutive tips of sleeve or gear as shown in Figure 4 and can be calculated by

$$y_{sg}max = 2\pi \times R/n_{dog} \quad (2)$$

where R is the sleeve or gear radius as shown in Figure 5 and n_{dog} is the number of dog teeth.

Teeth geometry parameters used in this paper are shown in Table 1.

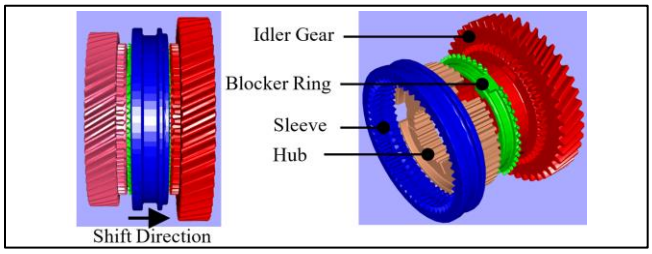

Figure 3 Mechanical Synchronizer

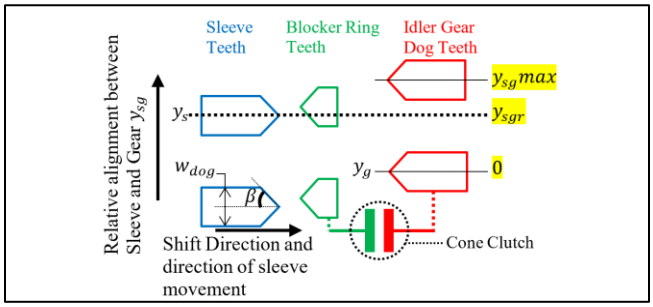

Figure 4 Synchronizer teeth in neutral position

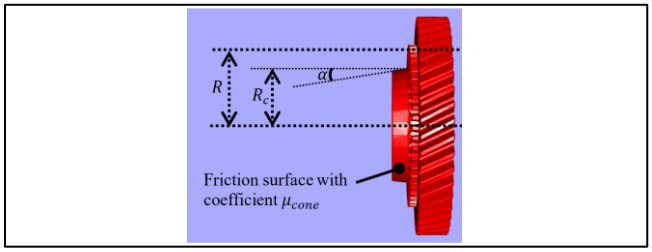

Figure 5 Cone clutch parameters

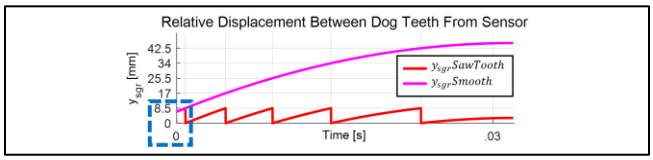

Figure 6 Sawtooth and Smoothened sensor signal

Table 1 Teeth Geometry parameters

Teeth Geometry Parameters	
w_{dog}	4 mm
$y_{sg}max$	8.5 mm
n_{dog}	45

It can be seen from [4] that y_s and y_g signals from sensor are sawtooth waves and $\in [0, y_{sg}max]$, so the resulting y_{sgr} will also be a sawtooth wave as shown in Figure 6 in red and

$$y_{sgr}(t_i) \in [0, y_{sg}max] \quad (3)$$

Since the signal $y_{sgr}(t_i)$ is used to calculate feedback signal, a smooth signal is preferred over a sawtooth signal. The smoothed signal is shown in magenta in Figure 6. Feedback signal for the relative angle between sleeve and gear θ_{sgr} can then be calculated by

$$\theta_{sgr} = y_{sgr}smooth/R \quad (4)$$

III. Speed Synchronization

Sleeve movement is in the shift direction in Figure 3. In Figure 2, it can be seen that synchronizer hub is connected to the wheels. Since sleeve is connected with synchronizer hub using spline coupling the sleeve speed ω_s can be calculated from drive shaft speed $\omega_{drive\ shaft}$ as

$$\omega_s = \omega_{drive\ shaft} \times Final\ Drive\ Ratio \quad (5)$$

where $\omega_{drive\ shaft}$ can be calculated using velocity of vehicle v_{veh} by

$$\omega_{drive\ shaft} = v_{veh}/R_w \quad (6)$$

where R_w is the radius of wheels and shift velocity v_{veh} for every gear shift is defined by ''Gear shift schedule'' as explained in [6].

In this paper it is assumed that v_{veh} remains constant during shift, which is a valid assumption since the vehicle does not have much time to decelerate if the shift is fast enough. So angular acceleration of sleeve α_s would be

$$\alpha_s = 0 \quad (7)$$

The synchronizer hub is connected with the blocker ring with rotary bump stops. So, blocker ring is mechanically connected to sleeve with a certain tangential clearance. The blocker ring is connected to idler gear by cone clutch. Before synchronization the speed of oncoming idler gear ω_g, hence forth referred to simply as idler gear, can be calculated as seen in Figure 2.

$$\omega_g(t \le t_0) = \omega_s \times (k1/k2) \quad (8)$$

where $k1$ and $k2$ are initial and target gear ratios respectively as shown in Figure 2.

When an axial force F_{ax} is applied on sleeve in the shift direction, the sleeve moves forward and makes contact with blocker ring teeth as shown in Figure 7. The time instance when sleeve teeth is in full contact with blocker ring teeth referred to as ''Blocking Position'' in [7] and is here denoted by time t_0. When sleeve is at blocking position the axial force F_{ax} applied on sleeve is transferred to the cone clutch speed and speed synchronization will start.

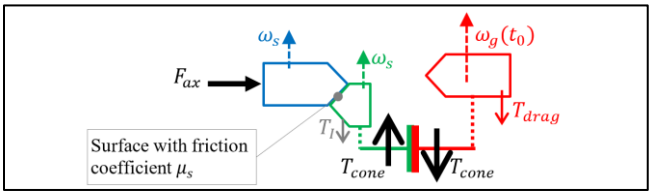

Figure 7 Sleeve at Blocking Position

If an upshift is considered then idler gear speed at the beginning of speed synchronization, $\omega_g(t_0)$ from (8) will be larger than sleeve speed ω_s from (5) as shown in Figure 7. The relation will be reversed for a downshift. Downshift is not considered in this paper, but the mathematical relations will be same and can be derived similarly. Additionally, for sake of simplicity, in this paper it is assumed that speed synchronization is done with cone clutch entirely. If the synchronization is done with either electric motor or with electric motor and cone clutch sequentially as shown in [1], the subsequent mathematical relations still hold but will need to include the synchronization torque from electric motor.

When the cone clutch is closed with a clamping force equal to axial force F_{ax}, a friction torque T_{cone} is generated as shown in Figure 7. T_{cone} can be calculated by

$$T_{cone} = F_{ax} \times \mu_{cone} \times R_c / \sin\alpha \quad (9)$$

where μ_{cone} is the friction coefficient of cone clutch, R_c is effective radius of cone and α is the cone angle as shown in Figure 5. In this paper F_{ax}, is considered to be constant and is the maximum axial force provided by the gear actuator.

The friction torque in a clutch will be in such a way that it will try to reduce the velocity difference between the plates. So, for an upshift, T_{cone} will try to reduce the speed of idler gear ω_g and increase ω_s since $\omega_g(t_0) > \omega_s$. Sleeve speed ω_s will not change since sleeve and blocker ring is connected to hub as shown in Figure 3 and hub is connected to wheels as shown in Figure 2, and thus the whole vehicle mass will act as a very large inertia on the sleeve. The idler has a smaller inertia stemming from its own mass, the input shaft and the electric motor. So, the idler gear velocity ω_g will decrease due to application of torque T_{cone} while the sleeve speed is constant.

For an upshift, the resulting angular acceleration of idler gear α_g can be calculated by

$$\alpha_g = (-T_{cone} - T_d)/J_g \quad (10)$$

where J_g is reflected moment of inertia of oncoming idler, input shaft [8] and electric motor [1]. T_d is drag torque on oncoming idler its value can be calculated by methods shown in [9]. In this paper drag torque is assumed to be a constant term so (10) can be re written as

$$\alpha_g = -(T_{synch})/J_g \quad (11)$$

Since T_{cone} and T_d in (10) are constants, T_{synch} in (11) is also a constant.

Idler velocity ω_g, after a time t_{synch}, ω_g becomes equal to ω_s. So

$$\omega_g(t_{synch}) - \omega_s = 0 \quad (12)$$

Relative velocity between sleeve and gear during speed synchronization $t \in [t_0, t_{synch}]$ is defined by $\omega_{sg}(t)$ where

$$\omega_{sg}(t) = \omega_g(t) - \omega_s \quad (13)$$

As it can be seen in Figure 7,that the sleeve is trying to push blocker ring from its path towards and go towards gear engagement by applying indexation torque T_I but cone torque T_{cone} is acting on the blocker ring in the opposite direction.

The expression of T_I from [10] is

$$T_I = F_{ax} \times R \times (1 - \mu_s \tan\beta)/(\mu_s + \tan\beta) \quad (14)$$

where μ_s is the friction coefficient of teeth surface and β is the half angle of teeth as shown in Figure 4. R is the sleeve or gear radius as shown in Figure 5.

To keep the sleeve stuck at blocking position until the condition in (12) is fulfilled, T_{cone} is always designed to be larger than T_I as mentioned in [10] so

$$T_{cone} > T_I \tag{15}$$

This design feature in (15) is very important as its fulfillment avoids clash and grating noise [10] .Normally T_{cone} is kept 3 times larger than T_I.

Since T_{cone} is a friction torque, when speed difference

$$\omega_{sg} \xrightarrow[approaches]{} 0 \xRightarrow[implies]{} T_{cone} \xrightarrow[approaches]{} 0 \tag{16}$$

Implication (16) is based on [11], which demonstrates the fact by calculating friction force against different slip velocities using various friction models.

Combining (16) with (12) and (13), it can be seen that relationship in (15) will only be reversed when ω_{sg} is nearly equal to zero at time t_{synch}, hence sleeve will be stuck at blocking position until $\omega_{sg} \cong 0$.

IV. Sleeve to Gear Engagement

Once speed synchronization is done at time t_{synch}, the sleeve moves towards idler gear as shown in Figure 8. When sleeve has moved a certain displacement x_{end}, the ramp up torque starts at time t_{end} as shown in Figure 8.

Relative alignment between sleeve and idler gear at synchronization time $y_{sg}(t_{synch})$ determines the trajectory of sleeve tip point during gear engagement as shown by purple and magenta curves in Figure 8. From Figure 8, it can be seen that if $y_{sg}(t_{synch})$ is equal to a particular value $y^*_{sg}(t_{synch})$, the sleeve teeth do not hit the idler gear dog teeth hence guarantying fastest gear engagement and least noise and wear. If, however gear engagement starts at another value as shown by the purple curve, the sleeve teeth will make a ''frontal contact'' which delays gear engagement and makes clonk noise and wear in the transmission.

So, it can be concluded that gear engagement must be started if and only if

$$y_{sg}(t_{synch}) = y^*_{sg}(t_{synch}) \tag{17}$$

[4] shows detailed calculation of $y^*_{sg}(t_{synch})$ and includes simulation results for verification.

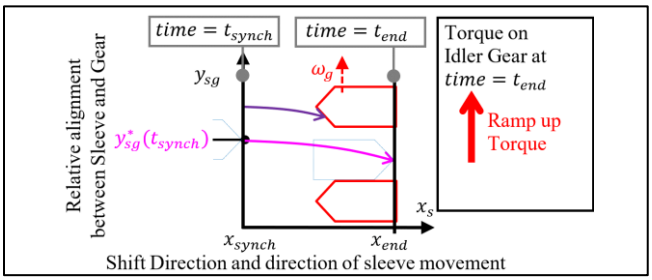

Figure 8 Sleeve to Gear engagement

V. Control Problem

The control problem can be formulated as

''Design a feedback controller that minimizes the time duration $t_{synch} - t_0$, *subject to* $y_{sg}(t_{synch}) = y^*_{sg}(t_{synch})$''

To use the existing approach to the solution of time optimal control problems as shown in [5], the problem should be expressed as a state-space model. So, two states x_1 and x_2 are introduced, for speed synchronization phase

$$x_1 = \theta_{sg};\ x_2 = \omega_{sg} \tag{18}$$

where θ_{sg} is the relative angle between sleeve and gear teeth.

From (18) it can be seen that

$$\dot{x_1} = x_2 \tag{19}$$

Based on (13)

$$\dot{\omega_{sg}} = \alpha_{sg} = \alpha_g - \alpha_s \tag{20}$$

Taking α_g and α_s from (11) and (7) , putting them in (20) and then using (18)

$$\dot{x_2} = \alpha_{sg} = -(T_{synch})/J_g \tag{21}$$

The state space model can then be written in matrix form using (18), (19) and (20) as

$$\begin{bmatrix}\dot{x_1}\\ \dot{x_2}\end{bmatrix} = \begin{bmatrix}0 & 1\\ 0 & 0\end{bmatrix}\begin{matrix}x_1\\ x_2\end{matrix} + \begin{bmatrix}0\\ 1\end{bmatrix}\alpha_{sg} \tag{22}$$

where α_{sg} is the input and it is constrained.

A. Constraints on Input

For speed synchronization during an upshift, done purely by cone clutch, the constraints on α_{sg} will be such that

$$-(T_{synch})/J_g \le \alpha_{sg} \le 0 \tag{23}$$

The upper limit of zero in (23) reflects the fact that a cone clutch can only decrease the speed difference ω_{sg} towards zero.

Since electric motor shown in Figure 2 can provide both a positive and a negative torque it can be used to increase the speed difference. If motor can provide a certain torque T_{em} at cone clutch in the direction opposite to T_{cone} as shown in Figure 7, ω_{sg} can be increased. So, (23) can be rewritten as

$$-(T_{synch})/J_g \le \alpha_{sg} \le T_{em}/J_g \tag{24}$$

where T_{em} and T_{synch} are not necessarily equal. It should be noted that T_{em} does not represent the motor torque used for synchronization as explained in [2]. T_{em} for the context of this paper is used to throw sleeve and gear out of synchronization by increasing ω_{sg}.

B. Boundary conditions on states

For state x_2 the boundary condition at time t_0 can be derived from subtracting (5) from (8) and the result will be a known constant denoted by ω_{sg0}. The boundary condition on x_2 at time t_{synch} is 0 as shown in (12).

x_1 at time t_0, denoted by θ_{sgr0} can be calculated using the measurement from the ''Dog teeth position sensor'' explained in [4]. If the relative alignment between sleeve and gear at time t_0 is $y_{sgr}(t_0)$ then θ_{sgr0} can be calculated by evaluating (4) at time t_0. Since $y_{sgr}(t_0)$ is bounded as shown by (3), $y_{sgr}smooth(t_0)$ will have same bounds because it can be seen from Figure 6 that both sawtooth and smooth signals have same value at time t_0. Consequently θ_{sgr0} will also be bounded.

For control system design θ_{sgr0} will be treated as an arbitrary but known bounded constant.

For state x_1 the boundary condition at time t_{synch} denoted by θ_{sgf} can be calculated using (17). So, boundary conditions can be summarized as

$$\begin{aligned} x_1(t_0) &= \theta_{sgr0} = \frac{y_{sgr}(t_0)}{R} \in [0, \frac{y_{sg}max}{R}] \\ x_1(t_{synch}) &= \theta_{sgf} = y^*_{sg}(t_{synch})/R \\ x_2(t_0) &= \omega_{sg0} \\ x_2(t_{synch}) &= 0 \end{aligned} \tag{25}$$

C. Defintion of control problem

Since the aim of feedback control is to minimize the time duration $t_{synch} - t_0$, the performance index J can be defined as

$$J = t_{synch} - t_0 \tag{26}$$

given

- state space model from (22)
- constraints on input α_{sg} from (24)
- boundary conditions on state variables in (25)

The Time optimal control problem solved in [5] has the same above-mentioned state space model, constraints, boundary conditions and performance index.

D. Optimal control sequences

By formulating the Hamiltonian as shown in [5] and then minimizing Hamiltonian according to Pontryagin Principle it follows that the time optimal control for this type of system must be of *''Bang Bang type''*.

The four optimal control sequences according to [5] will be

$$\{\lfloor\alpha_{sg}\rfloor\}\ OR\ \{\lceil\alpha_{sg}\rceil\}\ OR\ \{\lceil\alpha_{sg}\rceil, \lfloor\alpha_{sg}\rfloor\}\ OR\ \{\lfloor\alpha_{sg}\rfloor, \lceil\alpha_{sg}\rceil\} \tag{27}$$

where floor and ceiling functions in sequences shown in (27) correspond to limits of α_{sg} in (24). Since the state space in (22) is of 2nd order according to Theorem 7.3 in [5], the maximum number of switches in optimal control sequence is 1 as shown in (27).

It should be noted that the sequences in (27), correspond to both upshifts and downshifts. The reason is the state space in (22) and performance index (26) will be same for both upshifts and downshifts. Since Hamiltonian is derived from state space equations and performance index the optimal control sequences shown in (27) cover both cases.

The difference between an upshift and a down shift is then only in the constraints on input α_{sg} and boundary conditions. Since this paper only deals with upshifts the corresponding sequences will be

$$\{\lfloor\alpha_{sg}\rfloor\}\ OR\ \{\lceil\alpha_{sg}\rceil, \lfloor\alpha_{sg}\rfloor\} \tag{28}$$

The choice of these particular sequences becomes obvious, realizing that $\lfloor\alpha_{sg}\rfloor$ in (28) corresponds to $-(T_{synch})/J_g$in (24) and since for an upshift $\omega_g(t_0) > \omega_s$, implying that a negative acceleration must be applied to fulfill the corresponding boundary condition in (25). The sequence $\{\lceil\alpha_{sg}\rceil, \lfloor\alpha_{sg}\rfloor\}$, means that first a positive acceleration $\lceil\alpha_{sg}\rceil$ is applied which will increase ω_{sg} as explained earlier. $\lceil\alpha_{sg}\rceil$ is applied until a certain time and afterwards negative acceleration $\lfloor\alpha_{sg}\rfloor$ is applied make ω_{sg} decrease to 0.

Similar conclusion can be drawn when dealing with downshifts that the optimal control sequences will be either $\{\lceil\alpha_{sg}\rceil\}$ or $\{\lfloor\alpha_{sg}\rfloor, \lceil\alpha_{sg}\rceil\}$ with input constraints in (24) and boundary conditions in (25) updated to correspond with downshifts.

E. Switching Curve for $\lfloor\alpha_{sg}\rfloor$

The switching curve as defined by [5] is the phase plane trajectory which transfers any initial state to a particular final state. According to boundary conditions in (25), final state is $(\theta_{sgf}, 0)$.

According to the control sequences in (28), $\lfloor\alpha_{sg}\rfloor$ is the control signal that is connected to final state. The equation for the phase plane trajectory can be derived as follows.

Integrating both sides of (21)

$$x_2 = -\frac{T_{synch}}{J_g} \times t + c_2 \tag{29}$$

where c_2 is constant of integration.

In the following calculations constants are kept symbolic. Their exact values based on physical parameters are defined at the end of derivations.

From (29) value of integration time t, can be calculated as

$$t = (c_2 - x_2) \times J_g/T_{synch} \tag{30}$$

Putting value of x_2 from (29) in (19) and integrating both sides gives

$$x_1 = -\frac{1}{2} \times \frac{T_{synch}}{J_g} \times t^2 + c_2 \times t + c_1 \tag{31}$$

Putting value of t from (30) in (31), state x_1 can be written as function of state x_2

$$x_1 = -\frac{J_g}{2 \times T_{synch}} x_2^2 + \frac{J_g}{2 \times T_{synch}} c_2^2 + c_1 \tag{32}$$

Rewriting (32) by combining last two constants in a new constant c_3

$$x_1 = -\frac{J_g}{2 \times T_{synch}} x_2^2 + c_3 \tag{33}$$

Equation (33) represents a family of trajectories in the phase plane with an offset depending on c_3. The switching curve that is the trajectory connected to final state can be calculated by solving (33) for c_3, by putting $x_1 = \theta_{sgf}$ and $x_2 = 0$ which yields

$$c_3 = \theta_{sgf} \tag{34}$$

If boundary conditions are such that

$$y^*_{sg}(t_{synch}) = 4.245\ mm \tag{35}$$

$$\omega_{sg0} = 100\ rad/sec \tag{36}$$

and if T_{synch} is such that

$$-(T_{synch})/J_g = -1250\ rad/sec^2 \tag{37}$$

the switching curve is shown by dotted blue curve in Figure 9.

By the dotted blue curve Figure 9 it can be seen that if θ_{sgr0} is $= -239.3 \div R\ radians$ then the optimal control sequence will be $\lfloor\alpha_{sg}\rfloor$. If θ_{sgr0} is $< -239.3 \div R\ radians$ then the control sequence will be $\{\lceil\alpha_{sg}\rceil, \lfloor\alpha_{sg}\rfloor\}$. The offset

switching curve shown by solid blue curve in Figure 9, will be explained in the next section V.F.

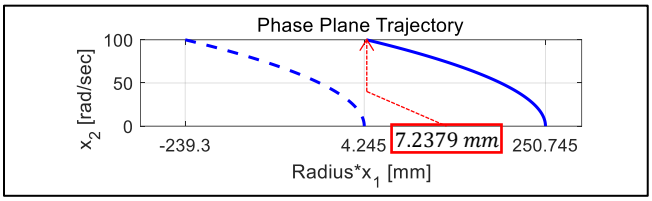

Figure 9 Switching Curve and offset switching curve for Upshift with $\lfloor\alpha_{sg}\rfloor$

F. Offsetting the switching curve

As θ_{sgr0} is lower bounded by zero as can be concluded from (3) and (4), it will lead to feedback signal at time t_0 being on the right side of the dotted switching curve shown in Figure 9. This situation must be avoided, and the reasoning is explained in subsequent section V.I. So, the switching curve must be offset with a constant c_4 such that

$$R \times \theta_{sgr0} + c_4 > 0 \tag{38}$$

where c_4 can be calculated by

$$c_4 = n \times y_{sg}max/R \tag{39}$$

where n is a positive integer.

So, (33) for switching curve for $\lfloor\alpha_{sg}\rfloor$ updated with new offset c_4 will be

$$x_1 = -\frac{J_g}{2\times T_{synch}} x_2^2 + c_3 + c_4 \tag{40}$$

The switching curve with offset is shown by solid blue curve in Figure 9. Constants c_3 and c_4 can be collected as a new constant c_5 such that

$$c_5 = c_3 + c_4 \tag{41}$$

So, switching curve (40) can be updated as

$$x_1 = -\frac{J_g}{2\times T_{synch}} x_2^2 + c_5 \tag{42}$$

Since n is an integer in (39), it can be verified that both $4.245\ mm$ and $250.745\ mm$ represent the same relative alignment between sleeve teeth and idler gear teeth with $n = 29$. Also, it can be seen from Figure 9, that c_5 is $250.745\ mm \div R\ radians$.

Relative alignment at ω_{sg0} is denoted by y_{sg1} and can be calculated by solving (42) at $x_2 = \omega_{sg0}$. So

$$y_{sg1} = R \times \left[-\frac{J_g}{2\times T_{synch}} \omega_{sg0}^2 + c_5\right] \tag{43}$$

Solving (43) results in $y_{sg1} = 7.2379\ mm$ which is marked by red rectangle in Figure 9.

G. Switching Curve $\lceil\alpha_{sg}\rceil$

The switching curve for $\lceil\alpha_{sg}\rceil$ is the curve that reaches final state of offset curve in Figure 9 i.e. $(c_5, 0)$ by applying a positive acceleration on the gear. The positive acceleration is T_{em}/J_g according to (24). The equation of curve calculated by using the procedure from section V.D will then be

$$x_1 = \frac{J_g}{2\times T_{em}} x_2^2 + c_5 \tag{44}$$

The complete switching curve is shown in Figure 10. The blue curve is for $\lfloor\alpha_{sg}\rfloor$ from (42) and red curve is for $\lceil\alpha_{sg}\rceil$ from (44). The difference in curvature is due to T_{synch} and T_{em} not being equal.

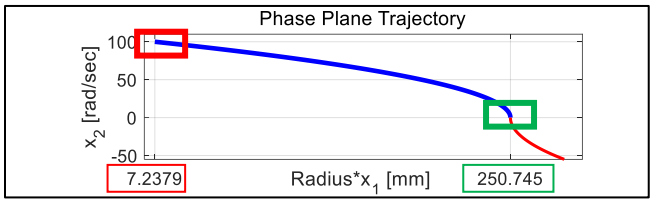

Figure 10 Complete switching curve

H. Feedback control

Using the switching curve in Figure 10, feedback controller can be designed that takes system from any initial state to the final state $(c_5, 0)$ by following the switching curve. The measurement for x_1 is θ_{sgr} as mentioned earlier and measurement for x_2 is ω_{sgr} and is from already existing speed sensors in the transmission. So

$$\begin{aligned} &Measured\ value\ of\ x_1 = \theta_{sgr} \\ &Measured\ value\ of\ x_2 = \omega_{sgr} \end{aligned} \tag{45}$$

Combining state measurements in (45) with switching curve (42) and (44), feedback law for time optimal control can be derived.

It can be seen for instance if $\omega_{sgr} > 0$ and $(\theta_{sgr}, \omega_{sgr})$ are such that they lie on the left blue curve in Figure 10, then α_{sg} must be $= \lceil\alpha_{sg}\rceil$ as explained in [5]. To check if $(\theta_{sgr}, \omega_{sgr})$ lie on the left of blue curve then the equation of the curve from (42) must be evaluated for $(\theta_{sgr}, \omega_{sgr})$. The condition can be formulated as

$$\theta_{sgr} + \frac{J_g}{2\times T_{synch}} \omega_{sgr}^2 - c_5 < 0 \tag{46}$$

which if $True \underset{implies}{\Longrightarrow} (\theta_{sgr}, \omega_{sgr})$ lies on the left of blue curve. So,

$$\begin{aligned} &\text{if } \theta_{sgr} + \frac{J_g}{2\times T_{synch}} \omega_{sgr}^2 - c_5 < 0\ AND\ \omega_{sgr} > 0 \\ &\quad \text{then } \alpha_{sg} = \lceil\alpha_{sg}\rceil \end{aligned} \tag{47}$$

By formulating different conditions such as condition (47) for different $(\theta_{sgr}, \omega_{sgr})$ for both curves in Figure 10 and then formulating the resulting optimal value for α_{sg}, the complete feedback control law for time optimal control is given by

$$\begin{aligned} &\text{if } \theta_{sgr} + \frac{J_g}{2\times T_{synch}} \omega_{sgr}^2 - c_5 > 0\ \ AND\ \omega_{sgr} > 0\ \ OR\ \ldots \\ &\text{if } \theta_{sgr} - \frac{J_g}{2\times T_{em}} \omega_{sgr}^2 - c_5 > 0 \quad AND\ \omega_{sgr} < 0\ \ OR\ \ldots \\ &\text{if } \theta_{sgr} - c_5 \geq 0\ AND\ \omega_{sgr} == 0 \\ &\qquad \textbf{then } \alpha_{sg} = \lfloor\alpha_{sg}\rfloor \\ &\textit{else} \\ &\text{if } \theta_{sgr} + \frac{J_g}{2\times T_{synch}} \omega_{sgr}^2 - c_5 < 0\ \ AND\ \omega_{sgr} > 0\ \ OR\ \ldots \\ &\text{if } \theta_{sgr} - \frac{J_g}{2\times T_{em}} \omega_{sgr}^2 - c_5 < 0 \quad AND\ \omega_{sgr} < 0\ \ OR\ \ldots \\ &\text{if } \theta_{sgr} - c_5 \geq 0\ AND\ \omega_{sgr} == 0 \\ &\qquad \textbf{then } \alpha_{sg} = \lceil\alpha_{sg}\rceil \end{aligned} \tag{48}$$

The top-level implementation of feedback control law in (48) is shown in Figure 11. It can be seen from control law in

(48), that $\alpha_{sg} = 0$ is not a solution as state space model in 22 is controllable as explained by Theorem 7.2 in [5].

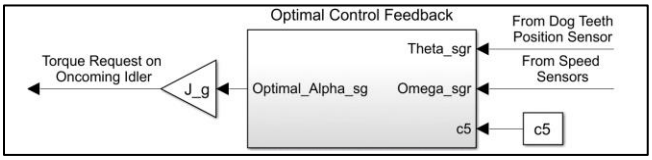

Figure 11 Implementation of feedback control law

Simulation results of the controller with $y_{sgr0} = [0, 2, 4, 6]\ mm$ are shown in Figure 12. Figure 12a, shows the zoomed in view around $\omega_{sg} = \omega_{sg0}$, marked by red rectangle in Figure 10. Figure 12b, is the zoomed in view around $\omega_{sg} = 0$, marked by green rectangle in Figure 10.

From Figure 12a, it can be seen that first $\lceil \alpha_{sg} \rceil$ is applied which increases the relative velocity between sleeve and gear x_2 to a certain level and then $\lfloor \alpha_{sg} \rfloor$ is applied until the end. It can be seen in Figure 12b that all the curves reach final state $(c_5, 0)$.

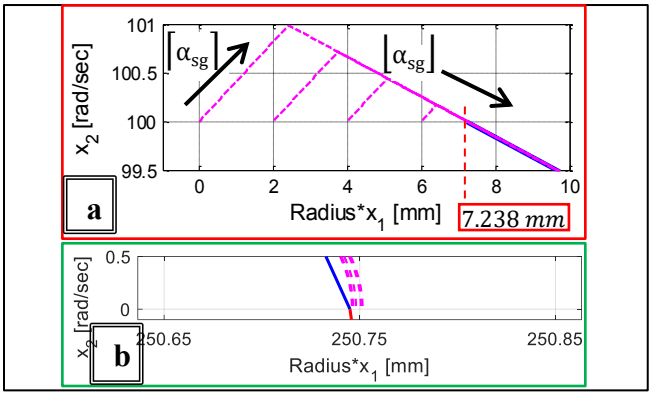

Figure 12 Time optimal control with $y_{sgr}(t_0) = 0; 2; 4; 6\ mm$

I. *Offsetting the switching curve based on initial conditions*

If y_{sgr0} is at its upper bound i.e. at $y_{sg}max$ according to (3), the simulation result is shown in Figure 13.

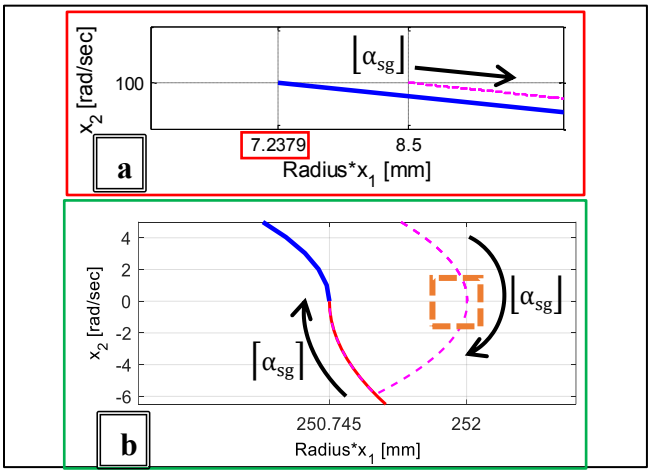

Figure 13 Time optimal control with $y_{sgr}(t_0) = 8.5\ mm$

Figure 13a, shows the zoomed in view around $\omega_{sg} = \omega_{sg0}$ and Figure 13b, is the zoomed in view around $\omega_{sg} = 0$, marked by red and green rectangles in Figure 10 respectively.

From Figure 13b it can be seen that the optimal control sequence in this case will be $\{\lfloor \alpha_{sg} \rfloor, \lceil \alpha_{sg} \rceil\}$, which is a part of optimal control sequences in (27) but not part of the optimal control sequence for an upshift in (28). It can be seen in Figure 13b that the final state $(c_5, 0)$ is reached in the simulation. But for synchronizer systems as explained earlier the implication in (16), will be fulfilled when x_2 approaches 0 as highlighted by orange square in in Figure 13b. Consequently, the torque relation in (15) will reverse and sleeve will leave the blocking position before $\lceil \alpha_{sg} \rceil$ is applied. The resulting final condition of x_2 will then be $252\ mm \div R\ radians$ as shown in Figure 13b. The resulting $y_{sg}(t_{synch})$ can be calculated to be $5.44\ mm$ according to [4], which is not equal to $y^*_{sg}(t_{synch})$ in (35).

The consequence of $y_{sg}(t_{synch})$ not being equal to $y^*_{sg}(t_{synch})$ according to [4] will be impacts between sleeve teeth and idler gear dog teeth and hence it is undesirable. To avoid this situation, the complete switching curve in Figure 10 must be offset such that

$$y_{sg1} \geq y_{sg}max \tag{49}$$

where y_{sg1} is defined by (43).

In order to fulfill the condition in (49), (43) must be updated with new offset c_6 so

$$y_{sg1} = R \times \left[-\frac{J_g}{2 \times T_{synch}} \omega^2_{sg0} + c_6 \right] \tag{50}$$

where

$$c_6 = c_5 + n_1 \times y_{sg}max/R \tag{51}$$

where n_1 is a positive integer. $(c_6, 0)$ will then be the new final state and the new offsetting can be summarized as

$$\begin{aligned} &\text{if } y_{sgr0} > y_{sg1} \\ &\text{then } c_5 \xrightarrow[is\ replaced\ by]{} c_6 \ \ in \\ &Curve\ equations\ 42\ and\ 43 \\ &and\ Feedback\ law\ equation\ set\ 48 \end{aligned} \tag{52}$$

The simulation result with new switching curves and new feedback law from condition in (52) is shown for $y_{sgr0} = y_{sg}max$ in Figure 14.

From Figure 14a it can be seen that updated $y_{sg1} = 15.738\ mm$ from (50), as opposed to $y_{sg1} = 7.238\ mm$ from (43). From Figure 14a, it can be seen that the control sequence is same as that in Figure 12 and is $\{\lceil \alpha_{sg} \rceil, \lfloor \alpha_{sg} \rfloor\}$. From Figure 14c, it can be seen that c_6 is $259.245\ mm \div R\ radians$. n_1 in (51) will then be in this particular case $= 1$. Also it can be verified that $259.245\ mm$ represents the same relative alignment between gear and sleeve teeth as $y^*_{sg}(t_{synch}) = 4.245\ mm$.

J. *Chatter in Time optimal Control*

According to [12] time optimal controllers of the type designed in this paper *chatter* i.e. the optimal control signal jumps between $\lceil \alpha_{sg} \rceil$ and $\lfloor \alpha_{sg} \rfloor$ rapidly near final state. The reason is when $(\theta_{sgr}, \omega_{sgr}) \rightarrow (c_5, 0)$ or $(c_6, 0)$, the

relational conditions in the feedback control law (48), change signs rapidly.

For synchronizer systems, this behavior can be eliminated for an upshift by turning the time optimal controller off and *latching* α_{sg} to a $\lfloor \alpha_{sg} \rfloor$, when $\omega_{sg} \cong 0$.

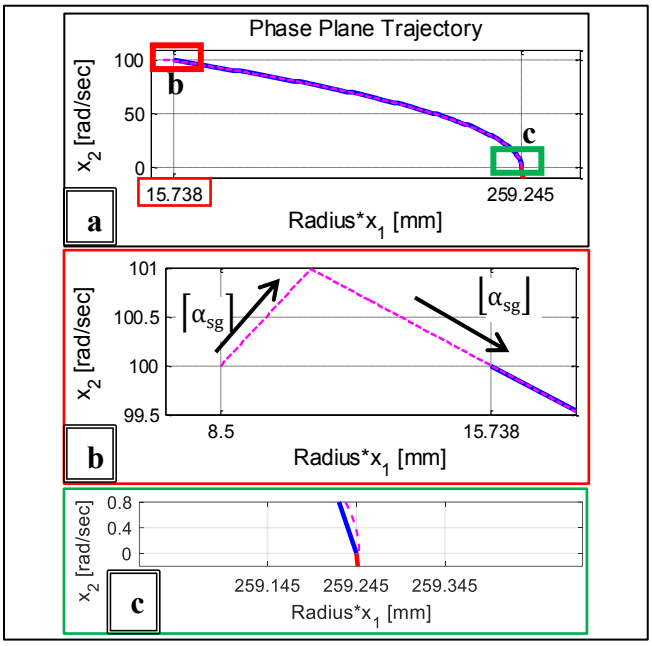

Figure 14 Time optimal control with $y_{sgr}(t_0) = 8.5\ mm$ with updated offset c_6

VI. Conclusions

In this paper a time optimal feedback control for synchronizer systems is designed and implemented in *Simulink*. The speed synchronization time and noise/wear during gear shifting are minimized. Speed synchronization can be done slightly faster if minimization of noise/wear is ignored. But the control algorithm given in this paper guarantees the fastest speed synchronization while fulfilling the criteria of reducing noise and wear. The results of the control algorithm are shown by simulations.

Although synchronizers can be modeled as double integrators, optimal control methods for double integrators cannot be applied to synchronizers straight away. The algorithms need modifications to be applicable on synchronizer systems. Several modifications have been derived and their inclusion in the algorithm has been demonstrated.

In this paper, the drag torque and synchronization torque are assumed to be constant during the gear shift. Development of time optimal control algorithms for variable torques will be a topic of future research.

The control method described in this paper is applicable to hybrid DCT and can be extended to dog clutch systems in general. The control method however is not applicable to conventional DCT because in conventional DCT the relative speeds can only be decreased.

VII. References

[1] M. Z. Piracha, A. Grauers and J. Hellsing, "Improving gear shift quality in a PHEV DCT with integrated PMSM," in *CTI Symposium Automotive Transmissions, HEV and EV Drives*, Berlin, 2017.

[2] A. Penta, R. Gaidhani, S. K. Sathiaseelan and P. Warule, "Improvement in Shift Quality in a Multi Speed Gearbox of an Electric Vehicle through Synchronizer Location Optimization," in *SAE Technical Paper*, 2017.

[3] Z. Lu, H. Chen, L. Wang and G. Tian, "The Engaging Process Model of Sleeve and Teeth Ring with a Precise, Continuous and Nonlinear Damping Impact Model in Mechanical Transmissions," in *SAE Technical Paper*, 2017.

[4] M. Z. Piracha, A. Grauers, E. Barrientos, H. Budacs and J. Hellsing, "Model Based Control of Synchronizers for Reducing Impacts during Sleeve to Gear Engagement," in *SAE Technical Paper*, Detroit, 2019.

[5] D. S. Naidu, Optimal Cotrol Problems, Pocatello, Idaho: CRC Press, 2003, pp. 293-314.

[6] T. S. Y. Z. Manish Kulkarni, "Shift dynamics and control of dual-clutch transmissions," *Elsevier Journal of Mechanism and Machine Theory,* no. 42, pp. 168-182, 2007.

[7] C.-Y. Tseng and C.-H. Yu, "Advanced shifting control of synchronizer mechanisms for clutchless automatic manual transmission in an electric vehicle," *Mechanism and Machine Theory,* vol. 84, pp. 37-56, 2015.

[8] H. Naunheimer, B. Bertsche, J. Ryborz and W. Novak, "Gearshifting Mechanisms," in *Automotive Transmissions: Fundamentals, Selection, Design and Application Second Edition*, Springer, 2011, pp. 310-334.

[9] K. M. H. Math and M. Lund, "Drag Torque and Synchronization Modelling in a Dual Clutch Transmission," CHALMERS UNIVERSITY OF TECHNOLOGY, Gothenburg, Sweden, 2018.

[10] S. T. Razzacki, "Synchronizer Design: A Mathematical and Dimensional Treatise," in *2004 SAE World Congress*, Detroit, 2004.

[11] A. S. S. B. Sören Andersson, "Friction models for sliding dry, boundary and mixed lubricated contacts," *Elsevier Tribology International,* no. 40, p. 580–587, 2007.

[12] V. G. Rao and D. S. Bernstein, "Naive Control of the double integrator," *IEEE Control Systems Magazine,* pp. 86-97, October 2001.